Organization and Metabolism of Plastids and Mitochondria in Arbuscular Mycorrhizal Roots of *Medicago truncatula*[1[w]]

Swanhild Lohse, Willibald Schliemann, Christian Ammer, Joachim Kopka, Dieter Strack, and Thomas Fester*

Leibniz-Institut für Pflanzenbiochemie, Abteilung Sekundärstoffwechsel, D–06120 Halle (Saale), Germany (S.L., W.S., C.A., D.S., T.F.); and Max-Planck-Institut für Molekulare Pflanzenphysiologie, 14476 Potsdam-Golm, Germany (J.K.)

Colonization of root cortical cells by arbuscular mycorrhizal fungi leads to marked cytological changes of plastids and mitochondria. Plastids in particular are forming tubular extensions partially connecting individual organelles in a network-like way. These cytological changes correspond to an increased need for plastid and mitochondrial products during establishment and functioning of the symbiosis. The analysis of metabolite and transcript levels in mycorrhizal and nonmycorrhizal roots from *Medicago truncatula* revealed concomitant changes regarding a number of metabolic pathways. Our results indicate the activation of the mitochondrial tricarboxylic acid cycle and of plastid biosynthetic pathways producing fatty acids, amino acids, and apocarotenoids. These observations provide a general overview of structural and metabolic changes of plastids and mitochondria during colonization of root cortical cells by arbuscular mycorrhizal fungi.

Arbuscular mycorrhiza (AM) is a mutualistic symbiosis between fungi from the order Glomales and roots of >80% of terrestrial plant species (Smith and Read, 1997). The cytological key feature of this interaction is the arbuscule, a haustorium-like fungal structure, forming a symbiotic interface within individual root cortical cells. Arbuscules are dynamic, short-living structures; they are thought to be involved in the transport of a number of nutrients (e.g. carbohydrates and phosphate). During formation of arbuscules, the volume of the plant cell cytosol, the size of the cell nucleus, and the number of the cell organelles increase, pointing to an activation of plant cell metabolism (Bonfante-Fasolo, 1984; Gianinazzi-Pearson, 1996). Plastids in particular are forming stromules (stroma filled tubules; for review, see Kwok and Hanson, 2004), leading to extensive network-like structures in the close vicinity of fungal arbuscules in roots of *Nicotiana tabacum* (Fester et al., 2001) and *Zea mays* (Hans et al., 2004). One special, and only poorly understood, feature of these plastids is the activation of carotenoid biosynthesis (Fester et al., 2002b), leading to the accumulation of various apocarotenoids (Fester et al., 2002a; Strack et al., 2003). Furthermore, it has been shown recently that the plastid-located proteins CASTOR and POLLUX are necessary for the entry of symbiotic bacteria (*Mesorhizobium loti*) and AM fungi into root cells of *Lotus japonicus* (Imaizumi-Anraku et al., 2005).

Nongreen plastids are important biosynthetic organelles. Metabolic pathways studied in recent years include *N*-assimilation (Esposito et al., 2003), starch biosynthesis (Geigenberger et al., 2004), and lipid biosynthesis (Schwender et al., 2004). There is an obvious need for a number of plastid products during the establishment and functioning of the AM symbiosis. Nevertheless, apart from apocarotenoid accumulation, no changes of plastid metabolism have been described in AM roots so far. We examined such changes by combining analyses of metabolite and transcript levels, including mitochondrial metabolism, which can supply ATP and carbon skeletons to the plastids (Mackenzie and McIntosh, 1999). We chose the AM model plant *Medicago truncatula* (Hause and Fester, 2004) for our analysis because the large amount of EST data available provides a good basis for the analysis of changes in transcript levels by electronic northern. The proliferation of organelles corresponding to the activation of mitochondrial catabolic and plastid anabolic pathways was analyzed by confocal laser scanning microscopy (CLSM) of AM roots containing organelles labeled with green fluorescent protein (GFP) after root transformation, mediated by *Agrobacterium rhizogenes*.

[1] This work was supported by the Deutsche Forschungsgemeinschaft (Bonn, Germany).

* Corresponding author; e-mail tfester@ipb-halle.de; fax 49–345–5582–1509.

[w] The online version of this article contains Web-only data.

Article, publication date, and citation information can be found at www.plantphysiol.org/cgi/doi/10.1104/pp.105.061457.

RESULTS

Plastid and Mitochondrial Structures in the Roots of *M. truncatula*

CLSM analysis of *M. truncatula* roots transformed with suitably targeted GFP showed that high numbers

of plastids and mitochondria are present within the central cylinder and only few of these organelles within the root cortex (Fig. 1, A, G, and I). In some cases, plastids were forming stromules within the central cylinder (Fig. 1D). AM colonization of roots led to the formation of arbuscules in the inner cortical cell layer (Fig. 1G) and to an increase in the numbers of plastids (Fig. 1, B and E) in the colonized cells. In single optical sections of cortical cells from noncolonized roots, we counted between 2 and 11 plastids (28 cells evaluated), and in single optical sections from colonized cells, 21 to 38 plastids could be observed. In some of these cells, individual plastids became connected by stromules (Fig. 1, C and F) resembling the plastid networks described for *N. tabacum* (Fester et al., 2001) and *Z. mays* (Hans et al., 2004). The connection of plastid metabolism and plastid shape is further demonstrated by plastids from transformed root explants, where plastids were virtually absent from the central cylinder and formed large roundish organelles in cortical cells (Fig. 1H).

In contrast to plastids, mitochondria are of essentially similar, highly variable shape in the central cylinder and in root cortical cells. Spherical forms of these organelles appeared to be more predominant in the root cortex, whereas thread-like forms were observed in particular within the central cylinder (Fig. 1K). Upon colonization of root cortical cells, mitochondrial shape was not changed significantly; however, we observed an increase of mitochondrial numbers and the aggregation of mitochondria in the vicinity of arbuscules (Fig. 1, J and L).

Transcript Levels of Key Metabolic Enzymes in AM Roots

A screening of The Institute for Genomic Research (TIGR) *Medicago truncatula* Gene Index (MtGI Release 7.0; http://www.tigr.org/tdb/tgi/mtgi/) for tentative consensus (TC) sequences connected to the metabolism of nongreen plastids, mitochondria, or to related cytosolic pathways resulted in about 700 sequences. Comparing the number of respective expressed sequence tags (ESTs) in cDNA libraries from mycorrhizal (in total 19,366 EST clones) and nonmycorrhizal (in total 18,783 EST clones) roots, we calculated likelihood ratios $R = L^1/L^0$ according to Journet et al. (2002). These ratios refer to the likelihood (L^1, L^0) of two hypotheses (H^1, H^0) calculated from the number of EST sequences observed in different libraries. In the null hypothesis H^0, the frequency of ESTs is constant, and different numbers of EST sequences are due to random variation. In the alternative hypothesis H^1, the frequency of EST sequences differs in the libraries examined. R-values therefore represent the probability for differential transcript levels regarding two tissues, here mycorrhizal and nonmycorrhizal roots, divided by the probability for identical levels of this transcript. Forty-six of the 700 sequences examined gave $R = 1.7$ and higher (Table I). Most of the annotations referred to enzymes of carbohydrate metabolism (including tricarboxylic acid [TCA] cycle and respiratory electron transport chain), followed by enzymes for the biosynthesis of amino acids and fatty acids. The percentage of TC sequences with elevated R-values was particularly high regarding carotenoid metabolism. Three TC sequences were annotated to corresponding enzymes, two of them with $R = 2.6$.

After elimination of TC sequences coding for identical enzymes and including TC85625, which is coding for a plastid-targeted isocitrate dehydrogenase and is characterized by a remarkably high number of EST clones in libraries from nonmycorrhizal roots when compared to mycorrhizal roots, we obtained 35 sequences for further analysis (Table I). For a number of these sequences, we observed considerably high numbers of EST clones in cDNA libraries from nodulated roots (comprising 21,371 EST clones in total; Table I). After aligning the putative proteins derived from the TC sequences with proteins of proven function, most TC sequences showed a high degree of sequence identity spanning the complete open reading frame (see Supplemental Table I). A missing similarity in the N-terminal regions of putative proteins in some cases may be explained by the presence of signal peptides for plastid or mitochondrial import.

Transcript levels of the 35 sequences (Table I) in mycorrhizal and nonmycorrhizal roots were measured using real-time RT-PCR. Primers defining 50-bp amplicons were selected from TC regions corresponding to the putative open reading frames (see Supplemental Table II). All primers were tested by conventional PCR and produced single products of the expected size. Analysis of melting behavior of the PCR product after real-time PCR revealed the existence of single PCR products. Standard curves for the various amplicons indicated high amplification efficiencies in all cases presented. In the case of six TC sequences, we did not succeed in selecting suitable primer pairs. These sequences were excluded from the subsequent analyses. Difference of cycle threshold (Δc_t)-values were calculated by subtracting mean c_t-values of assays from mycorrhizal roots from the respective mean c_t-values of assays from nonmycorrhizal roots. An amplicon corresponding to the plant translation elongation factor (*EF*) 1α was used for internal standardization by substracting the Δc_t-value for this amplicon from the Δc_t-values of the various samples resulting in $\Delta\Delta c_t$-values. The Δc_t-values regarding this amplicon showed only a minor variation (Δc_t ranging from -0.25–0.45), indicating the use of comparable amounts of cDNA. The amplicon corresponding to the mycorrhiza-specific phosphate transporter (*MtPT4*) from *M. truncatula* (Harrison et al., 2002) was used as a control for the existence of a functional mycorrhizal symbiosis (Isayenkov et al., 2004) and for the presence of functionally active arbuscules in particular. $\Delta\Delta c_t$-Values regarding this amplicon were ranging between 8.4 (roots harvested 30 d after inoculation) and 9 or 12 (roots harvested 60 d after inoculation),

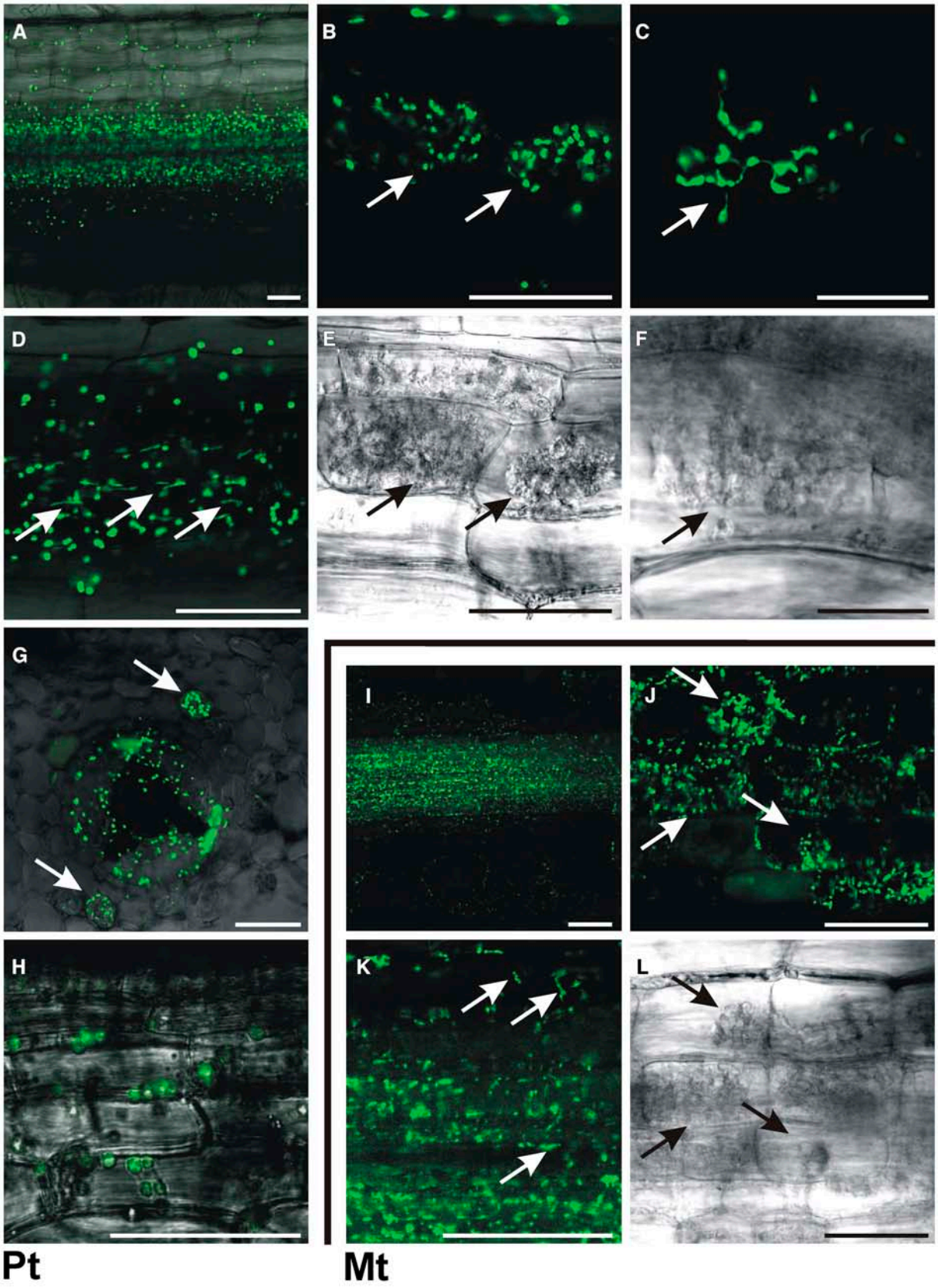

Figure 1. Bright-field micrographs and green fluorescence according to CLSM analysis of plastids (A–H) and mitochondria (I–L) labeled by the GFP in mycorrhizal and nonmycorrhizal roots from *M. truncatula*. Longitudinal sections of nonmycorrhizal roots reveal large amounts of plastids (A) and mitochondria (I) within the central cylinder. Corresponding details show stromules of

indicating a high percentage of functional mycorrhizal colonization that corresponded to the microscopically determined degrees of mycorrhizal colonization (colonized roots/whole root system) of approximately 30% (roots harvested 30 d after inoculation) and 70% (roots harvested 60 d after inoculation). The group of plants showing the highest $\Delta\Delta c_t$-value for the *MtPT4* amplicon gave the highest $\Delta\Delta c_t$-values for most amplicons. The plants harvested 30 d after inoculation with a colonization degree of approximately 30% and a $\Delta\Delta c_t$-value for the *MtPT4*-amplicon of 8.4, in contrast, gave the lowest $\Delta\Delta c_t$-values for most amplicons.

Roots harvested 90 d after inoculation showed a high degree of mycorrhizal colonization (approximately 80%), a Δc_t-value for the *EF* amplicon of 1.5, and a $\Delta\Delta c_t$-value for the *MtPT4* amplicon of 9.5. $\Delta\Delta c_t$-values for the amplicons tested, however, were quite low. Only in the case of TC78514 (ζ-carotene desaturase), TC79399 (enoyl-acyl carrier protein [ACP] reductase), and TC76985 (pyruvate decarboxylase) did $\Delta\Delta c_t$-values reach approximately 1.

Amplicons representing enzymes for amino acid and fatty acid biosynthesis as well as for carotenoid metabolism showed significantly and repeatedly elevated $\Delta\Delta c_t$-values regarding the plants harvested 60 d after inoculation. In most cases, $\Delta\Delta c_t$-values regarding the plants harvested 30 d after inoculation were elevated as well. $\Delta\Delta c_t$-values for these amplicons are summarized in Table I. Regarding amino acid biosynthesis, two of the TC sequences found are annotated to enzymes involved in the assimilation of ammonia and the production of Asn (Asp transaminase and Asn synthase), a major plant storage and transport compound for nitrogen. The third TC sequence is annotated to anthranilate phosphoribosyl transferase, catalyzing the second committed step of Trp biosynthesis. Regarding fatty acid biosynthesis, TC sequences with elevated transcript levels in AM roots have been found for a subunit of the acetyl-CoA carboxylase complex (ACCC) as well as for the ACP *S*-malonyl transferase and the enoyl-ACP reductase. Referring to the metabolism of carotenoids, only three TC sequences had been found by in silico analysis, two of them are characterized by R-values of 2.6 and $\Delta\Delta c_t$-values of about 1. These TC sequences are annotated as ζ-carotene desaturase and as a carotenoid cleaving enzyme. The first of these enzymes is involved in providing lycopene, the precursor of most other carotenoids, and the second enzyme is responsible for the oxidative cleavage of carotenoids (Schwartz et al., 2001) leading to carotenoid degradation products comparable to those described repeatedly for AM roots (Fester et al., 2002a).

In summary, our analysis clearly shows an increase in transcript levels referring to enzymes of amino acid and fatty acid biosynthesis as well as carotenoid metabolism. Regarding carbohydrate metabolism, similar increases in transcript levels were predicted by in silico analysis, but were not observed by real-time RT-PCR.

Steady-State Levels of Metabolites in AM Roots

Steady-state levels of polar metabolites from mycorrhizal and nonmycorrhizal roots from *M. truncatula* harvested 40 d after inoculation with the AM fungus have been determined using gas chromatography-mass spectrometry (GC-MS) metabolite profiling analysis (Fig. 2A). Regarding polar metabolites, about 170 compounds were identified (the complete data set is given in Supplemental Table III). About 50 of these compounds accumulated to different levels in mycorrhizal and nonmycorrhizal roots, most notably various sugars and sugar alcohols (anhydrosorbitol, Fru, Fuc, galactinol, glycerol, gulose, maltose, maltotriose, mannitol, melezitose, melibiose, *myo*-inositol, rhamnose, Suc, trehalose, and Xyl), organic acids, and amino acids (acetylglutamate, Ala, aminoadipate, aminobutyrate, Arg, Asp, Asn, Cys, dehydroascorbate, ferulate, fumarate, Glu, Gln, indol-3-acetate, Lys, malate, maleate, Orn, Pro, pyroglutamate, Tyr, and Trp). In this publication, we focus on compounds referring to plastid and mitochondrial metabolism and on phosphate and trehalose, which are directly linked to a functional mycorrhizal symbiosis (Table II). Apart from clear increases in phosphate levels and from the presence of trehalose in AM roots, we observed significant increases in the levels of the amino acids Asp, Glu, Gln, Lys, Arg, and Cys and lower increases in the levels of Asn, Tyr, and Trp. In addition, two compounds involved in the mitochondrial TCA cycle, fumarate and malate, markedly decreased.

Steady-state levels of nonpolar metabolites from mycorrhizal and nonmycorrhizal roots from *M. truncatula* harvested 40 d after inoculation with the AM fungus have been determined using a different extraction procedure and GC-time of flight (TOF)-MS analysis (Fig. 2B). Most differentially accumulating compounds were identified as fatty acids using authentic reference substances. A significant increase of

Figure 1. (*Continued.*)
plastids (D, see arrows) and thread-like mitochondria (K, see arrows). The cross section of a mycorrhizal root from *M. truncatula* (G) allows a comparison between the occurrence of plastids within the central cylinder and within a colonized cell from the inner cortex (see arrows). Plastids from transformed root explants show large, roundish forms (H). Regarding the micrographs presenting colonized cells (B, C, E, F, J, and L), green fluorescence (B, C, and J) and bright-field micrographs (E, F, and L) are given separately, and arbuscules are marked by arrows. Plastids in such cells are strongly proliferating (B) and forming connecting stromules in some cases (C); mitochondria are proliferating and forming more or less clumped aggregates (J). All bars represent 50 μm, except for C and F, which represent 20 μm.

Table I. *In silico and real-time RT-PCR analysis of transcript levels of M. truncatula TC sequences*

The table summarizes R- and $\Delta\Delta C_T$-values of TC sequences with R > 1.7. R-values were obtained by comparing EST numbers in cDNA libraries from mycorrhizal (M) and (NM) nonmycorrhizal roots. They represent the probability for differential transcript levels regarding two tissues divided by the probability for identical levels. The number of EST clones found in cDNA libraries from nodulated roots (Nod) is given in parentheses. $\Delta\Delta c_t$-Values result from relative quantification (referring to the constitutively expressed translation elongation factor 1α) of real-time RT-PCR analyses regarding two independent batches of mycorrhizal and nonmycorrhizal plants, harvested 60 d after inoculation. Results from plants harvested 30 d after inoculation, and consequently less colonized, are given in parentheses in the cases analyzed. TC85523, 87062, 86522, 85559, 89116, and 85632 could not be analyzed due to problems defining suitable primer pairs and are marked as not determined (n.d.). $\Delta\Delta c_t$-Values indicating elevated transcript levels in AM roots are marked in bold. ACC, Acetyl-CoA carboxylase; ACP, acyl carrier protein; anthranilate PR transferase, anthranilate phosphoribosyl transferase; CCD, carotenoid 9,10 (9′,10′) cleaving dioxygenase; cyt, cytosolic; mt, mitochondrial; NDP, nucleoside diphosphate; SOD, superoxide dismutase.

TC	Protein	M/NM (Nod)	R-Value	$\Delta\Delta c_t$
Carbohydrate metabolism				
TC89468	Fru-1,6-bisphosphatase	3/0 (0)	2.6	0.4/−0.1
TC85625	Isocitrate dehydrogenase (cyt)	7/21 (11)	10.5	0.2/−0.4
TC76834	Isocitrate dehydrogenase (mt)	7/2 (22)	1.9	0.2/0.2
TC87405	6-Phosphogluconate dehydrogenase	5/0 (0)	7.3	0.2/−1.0
TC76985	Pyruvate decarboxylase	8/0 (8)	34.0	0.4/−0.5
TC85523	Respiration, complex I	9/2 (4)	3.7	n.d.
TC87062	Respiration, complex III	5/0 (5)	7.3	n.d.
TC86522	Respiration, complex IV	6/1 (3)	2.8	n.d.
TC86395	Succinate-CoA ligase	7/0 (1)	20.0	0.8/−0.3 (0.2)
TC87174	Succinate-CoA ligase	6/1 (1)	2.8	0.3/0.2
TC78918	Suc synthase	5/0 (0)	7.3	0.8/0.0
TC85400	Suc synthase	45/17 (67)	48.0	0.6/0.3
TC85632	Transaldolase	12/4 (6)	2.9	n.d.
Amino acid biosynthesis				
TC87326	Anthranilate PR transferase	4/0 (0)	4.4	**1.9/1.0 (0.3)**
TC85436	Asn synthetase (cyt)	11/1 (19)	22.0	**2.0/0.2 (0.9)**
TC77230	Asparaginase	3/0 (6)	2.6	0.2/−0.8
TC86066	Asp transaminase	5/1 (6)	1.9	**1.9/1.2 (0.9)**
TC85944	Asp transaminase (cyt)	8/0 (5)	34.0	0.2/−0.1
TC77163	Chorismate synthase	3/0 (0)	2.6	0.6/−0.4
TC76602	Cysteine synthase	6/1 (1)	2.8	0.8/−1.4 (0.1)
TC76943	Gln synthetase (cyt)	13/5 (5)	2.4	0.5/0.3
TC86783	Shikimate kinase	5/1 (0)	1.9	−0.4/−0.4
Fatty acid biosynthesis				
TC88181	ACCB	3/0 (1)	2.6	1.5/0.5
TC86279	ACCC	7/2 (0)	1.9	**1.3/0.9 (0.8)**
TC85559	ACCD	10/4 (1)	1.7	n.d.
TC77871	ACP *S*-malonyltransferase	6/0 (0)	12.0	**2.0/1.3 (0.5)**
TC79399	Enoyl-ACP reductase	4/0 (0)	4.4	**1.7/1.1 (0.7)**
Carotenoid metabolism				
TC78514	ζ-Carotene desaturase	3/0 (1)	2.6	**1.3/1.3 (0.0)**
TC77454	CCD	3/0 (1)	2.6	**1.5/1.0 (0.5)**
Various transcripts				
TC89116	Argininosuccinate synthase	3/0 (1)	2.6	n.d.
TC76898	Dehydroascorbate reductase	5/0 (5)	7.3	0.2/−0.8
TC77009	Ferritin	14/0 (5)	741.0	1.0/−1.0 (0.2)
TC87275	Fe-SOD	5/0 (0)	7.3	1.0/0.2 (−1.0)
TC77125	Immunophilin	11/2 (9)	7.5	0.2/−1.0
TC85556	NDP kinase	16/4 (26)	9.5	−0.4/−0.4

metabolite levels in AM roots was observed in the case of palmitate, oleate, and stearate (Table II). In addition, increases in linolenate and linoleate levels were also observed. Palmitvaccenoate and vaccenoate appeared as fungus-specific compounds in AM roots.

DISCUSSION

The massive proliferation of plastids in colonized root cortical cells from *N. tabacum* (Fester et al., 2001) and *Z. mays* (Hans et al., 2004) suggested a crucial role for these organelles. Increased amounts of products

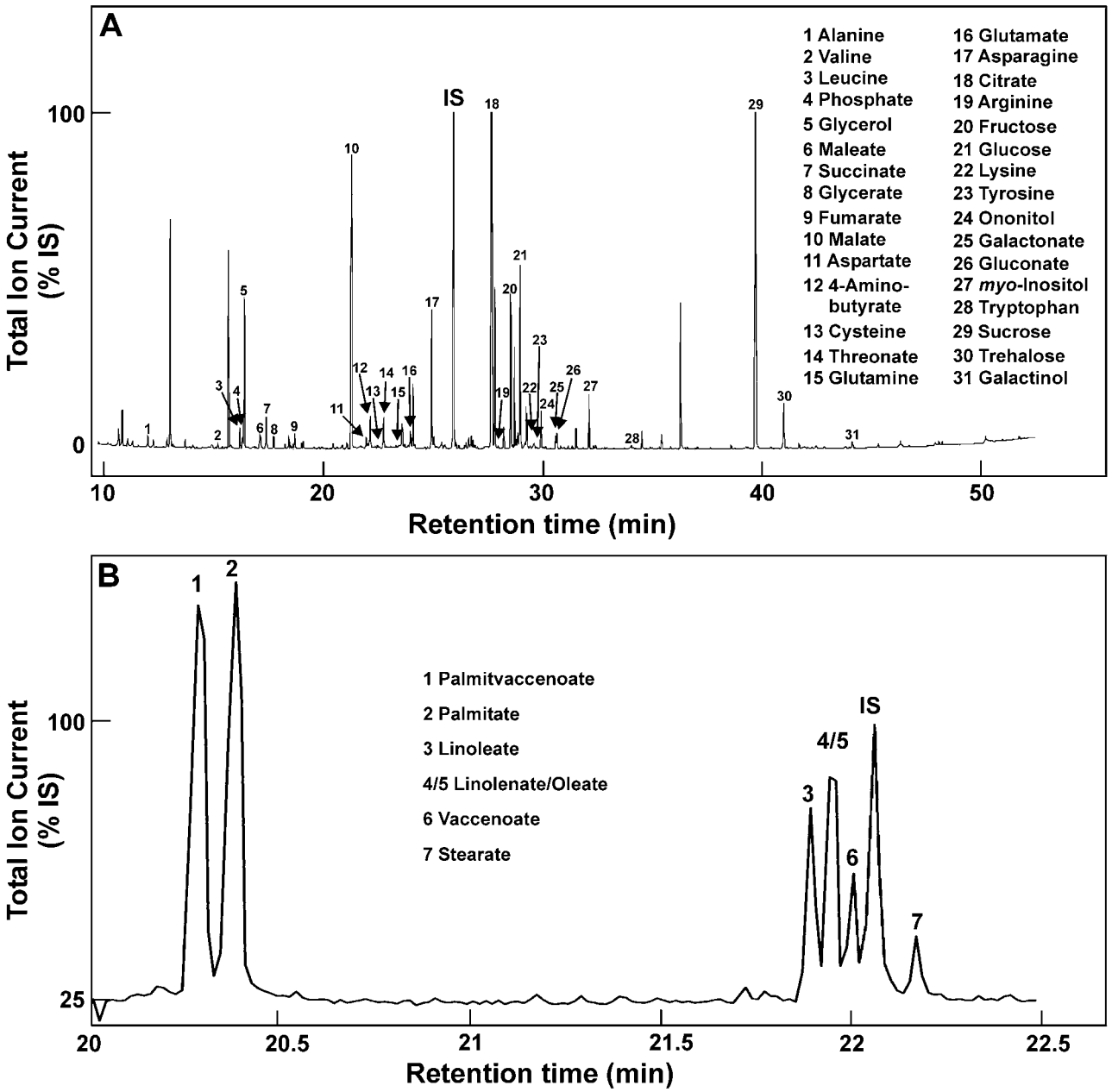

Figure 2. Representative GC-MS profile of polar (A) and GC-TOF-MS profile of nonpolar (B) metabolites from mycorrhizal *M. truncatula* root samples harvested 40 d after inoculation. Metabolites were identified using specific mass fragments and validated by the Automated Mass Spectral Deconvolution and Identification System in (A) and using authentic reference substances in (B). Regarding polar metabolites, only a part of the metabolites identified is indicated. The complete data set is given in Supplemental Table III. Regarding nonpolar metabolites, only the part of the chromatogram with signals from fatty acids is presented. A quantitative comparison of metabolite levels in mycorrhizal and nonmycorrhizal roots using ribitol (polar metabolites) and methyl nonadecanoate (nonpolar metabolites) as internal standards (IS) and referring to metabolites relevant for plastid or mitochondrial metabolism is given in Table II.

from plastid biosynthetic pathways (e.g. fatty acids or amino acids) are necessary to allow the formation of symbiotic structures (e.g. the periarbuscular membrane) and to support the general increase in metabolic activity. To detect corresponding metabolic changes, we examined plastid biosynthetic activity in AM roots of the model plant *M. truncatula*. Mitochondria were included in this analysis because they are providing ATP and carbon skeletons for plastid metabolism.

The Identification of Metabolic Changes in AM Roots

Possibly differentially accumulating transcripts were selected in a first screen by electronic northern

Table II. *Levels of polar and nonpolar metabolites from mycorrhizal (M) and nonmycorrhizal (NM) roots of M. truncatula harvested 40 d after inoculation*

Only differentially accumulating metabolites relevant for plastid or mitochondrial metabolism are listed. Polar metabolites were analyzed by GC-MS-based metabolite profiling of methoxyaminated and trimethylsilylated derivatives. Nonpolar metabolites were analyzed by GC-TOF-MS-based metabolite profiling of trimethylsilylated derivatives. Representative chromatograms are given in Figure 2; the complete data set regarding polar metabolites is given in Supplemental Table III. Metabolites are represented by specific mass fragments that are characterized by mass-to-charge ratio (*m/z*), by the retention time index (RI), and by the difference between measured and expected RI (ΔRI). These fragments were used for the quantification of each metabolite after normalization to internal standards (ribitol and methyl nonadecanoate, respectively). Replicate analyses ($n = 3$) were performed referring to three independent biological samples of mycorrhizal and nonmycorrhizal roots. The relative SD (%SD) of measurements is in parentheses. Unless indicated otherwise, Student's *t* test resulted in $P \leq 0.05$. Metabolites marked as undetected (u.) in (NM) roots are exclusively produced by the fungus; the other metabolites are produced by both symbiotic organisms. n.d., Not determined.

Metabolite	Fragment (*m/z*)	RI	ΔRI	Response NM (SD)	Response M (SD)	Response Ratio (M/NM)
Polar metabolites						
Phosphate	314	1,272.24	−5.6	0.33 (168)	3.95 (33)	12.00
Trehalose	169	2,734.50	−15.3	u.	6.35 (24)	–
Arg	157	1,827.20	−5.2	1.46 (9)	5.97 (10)	4.10
Asn[a]	258	1,678.10	−4.3	11.81 (28)	33.65 (52)	2.85
Asp	232	1,516.20	−9.0	6.93 (27)	11.24 (17)	1.62
Cys	220	1,558.10	−2.6	1.72 (17)	12.41 (20)	7.20
Fumarate	217	1,354.90	−4.0	0.25 (35)	0.10 (19)	0.41
Glu	246	1,623.10	−8.6	5.80 (18)	17.58 (25)	3.03
Gln	156	1,779.80	−4.8	0.06 (41)	0.30 (44)	5.32
Lys	174	1,914.40	−7.1	1.13 (38)	2.19 (22)	1.93
Malate	335	1,486.30	−5.4	43.69 (30)	20.45 (16)	0.47
Tyr[a]	280	1,932.30	−8.8	0.08 (52)	0.18 (43)	2.35
Trp[a]	202	2,206.20	−10.9	1.89 (43)	3.93 (39)	2.08
Nonpolar metabolites						
Palmitvaccenoate	311	n.d.		u.	430 (15)	–
Vaccenoate	339	n.d.		u.	96 (34)	–
Linolenate[b]	335	n.d.		23 (44)	46 (32)	2.0
Linoleate[a]	337	n.d.		44 (23)	92 (34)	2.1
Oleate	339	n.d.		8 (17)	68 (23)	8.6
Palmitate	313	n.d.		230 (10)	610 (19)	2.7
Stearate	341	n.d.		35 (12)	71 (14)	2.0

[a] $P \leq 0.15$ (Student's *t* test). [b] $P \leq 0.07$ (Student's *t* test).

analysis prior to a closer analysis by real-time RT-PCR. Whereas only few differentially accumulating transcripts connected to primary metabolism have been observed in AM roots using cDNA arrays for transcript profiling (Liu et al., 2003), electronic northern analysis resulted in a number of sequences that could be analyzed further.

There are a number of problems when analyzing metabolic changes in AM roots: (1) Our measurements refer to whole root systems, containing relatively small numbers of colonized cells (Fig. 1G) of varying symbiotic state. Accordingly, our analysis underestimates the actual changes regarding transcript and metabolite levels in individual colonized cells.

(2) Transcript levels referring to primary metabolism may depend on various external factors, possibly explaining the poor correlation between a number of R- and $\Delta\Delta c_t$-values. The TC sequences annotated to Asp transaminase and ACCC, example given, were characterized by small R-values (1.9 each) but had clearly elevated transcript levels in AM roots according to real-time RT-PCR. Other TC sequences with high R-values like ferritin (741), Suc synthase (48), or pyruvate decarboxylase (34) were apparently not induced in our plants according to real-time RT-PCR.

(3) A further problem regards the interpretation of metabolite data. Whereas the plant origin of apocarotenoids (Walter et al., 2000) and some fatty acids (Olsson, 1999) as well as the predominant fungal origin of trehalose (Douds et al., 2000) and a different set of fatty acids (Olsson, 1999) have been shown before, it is impossible to determine the biosynthetic origin of individual intermediates of carbohydrate catabolism or amino acid biosynthesis. Nevertheless, the observation of concomitant changes of metabolite and transcript levels regarding individual enzymatic steps allows the identification of metabolic pathways apparently induced in colonized roots (Fig. 3). Thus, our data provide a comprehensive view of the

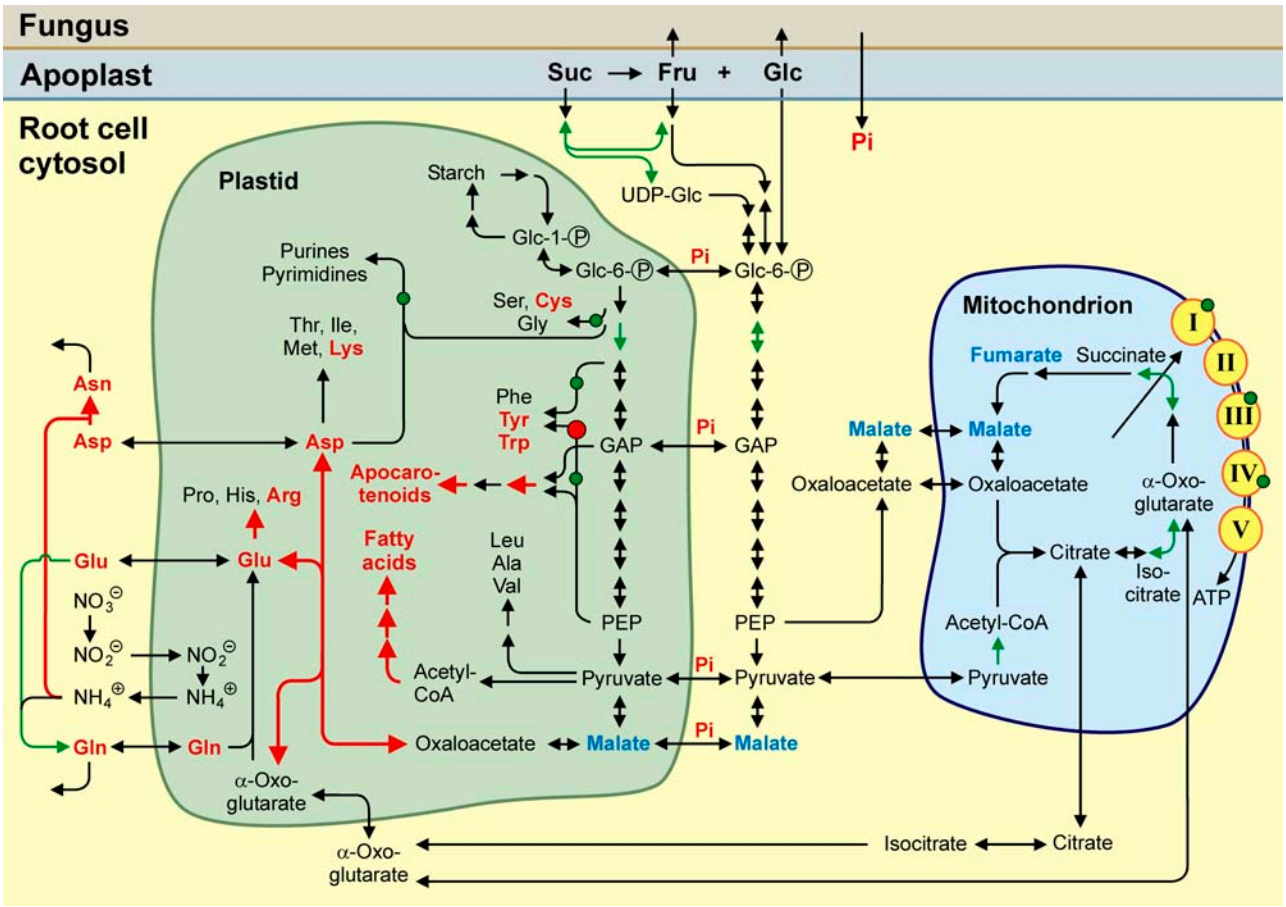

Figure 3. Complementary changes of transcript and metabolite levels indicating the activation of mitochondrial TCA cycle and of plastid biosynthetic pathways producing fatty acids, amino acids, and apocarotenoids. Enzymatic steps referring to TC sequences with significantly more EST clones in cDNA libraries from mycorrhizal when compared to nonmycorrhizal roots ($R > 1.7$) are marked in green. Confirmation of differential transcript levels by real-time RT-PCR is indicated by bold red arrows or red dots. Metabolites showing increased amounts in mycorrhizal roots are marked in red, and metabolites with decreased amounts are shown in blue. Increased amounts of metabolites might partially be due to fungal biosynthetic activity (see discussion). PPP, Pentose phosphate pathway; PEP, phosphoenolpyruvate; GAP, glycerinaldehyde 3-P.

metabolic reactions of roots to the colonization by AM fungi.

Metabolic Pathways Induced in AM Roots

According to GC-MS analysis, the levels of amino acids such as Asp, Glu, Gln, Lys, Arg, Cys, Asn, Tyr, and Trp are increased in AM roots. The increasing levels of these metabolites are accompanied by increasing levels of plant transcripts for key biosynthetic enzymes like Asp aminotransferase, Asn synthase, and anthranilate phosphoribosyl transferase.

In the case of fatty acids, plants and AM fungi are producing different sets of metabolites. Palmitvaccenoate and vaccenoate are typical fungal fatty acids, and palmitate, linoleate, and linolenate are of predominant plant origin (Olsson, 1999). Increasing levels of both groups of metabolites are the result of active plant and fungal fatty acid biosynthesis. The activation of plant fatty acid biosynthesis is further confirmed by finding increased transcript levels for key enzymes of this pathway (acetyl-CoA carboxylase, ACP *S*-malonyl transferase, and enoyl-ACP reductase).

Regarding apocarotenoid biosynthesis, both fragments derived from carotenoid oxidative cleavage can be detected photometrically in *M. truncatula* by HPLC (Fester et al., 2002a, 2005) but were not detected by the methods used here. In addition, the AM-dependent activation of the methylerythritol-P pathway (Walter et al., 2000) and of carotenoid biosynthesis (Fester et al., 2002b) has been demonstrated for *M. truncatula*. These earlier reports are now supported by finding AM-responsive transcripts with sequence similarity to a further enzyme involved in carotenoid biosynthesis (ζ-carotene desaturase) and to a carotenoid cleaving dioxygenase producing the fragments observed in AM roots (Schwartz et al., 2001; Fester et al., 2002a).

Regarding mitochondrial metabolism, we observed a decrease of fumarate and malate, two metabolites of the TCA cycle. Fumarate in particular is exclusively assigned to the TCA cycle, while malate is also involved in transport systems between the cytosol and

mitochondria or plastids. The finding of reduced steady-state levels of these two compounds is indicative most likely for an increased activity of the TCA cycle. This conclusion is supported by positive in silico results for a number of respective TC sequences. Regarding the activation of other pathways of carbohydrate catabolism (glycolysis or the pentose phosphate pathway [PPP]), only few in silico and no experimental data were obtained. Because products of these pathways, however, are necessary for building up fatty acids and carotenoids, a respective activation in AM roots appears likely.

Functional Significance of the Metabolic Changes Observed

The cellular changes observed during the formation of arbuscules suggest a general activation of plant cell metabolism (Bonfante-Fasolo, 1984; Gianinazzi-Pearson, 1996). This activation results in a higher demand for most products of plastid metabolism, including nucleotides, amino acids, and fatty acids. In agreement with our findings, fatty acids can be predicted to be of particular importance. Building up the periarbuscular membrane, colonized cells are increasing twofold to fourfold the surface of their plasma membrane (Bago et al., 2000). In addition, intracellular membrane systems, e.g. plastid, mitochondrial, or endoplasmic reticulum membranes (Hause and Fester, 2004), are proliferating as well. In contrast to this, the prominent position of the biosynthetic pathway leading to Asp and Asn (Fig. 3) reflects either an increasing demand for protein biosynthesis or the ability of AM fungi to provide nitrogen to their host plants (Hodge et al., 2001) and the use of Asn as a major compound for storage and transport of nitrogen in *M. truncatula*. The latter process might involve plastids from the central cylinder as well as plastids from colonized root cortical cells. Finally, the functional meaning of apocarotenoid biosynthesis has not been explained so far (Strack et al., 2003), although such compounds are accumulating in AM roots from a large variety of plants, in some cases to considerable levels (Fester et al., 2002a, 2005), and the induction of respective enzymes has been shown in a number of cases (Walter et al., 2000; Fester et al., 2002b; Hans et al., 2004). Recent experiments suggest a connection of this phenomenon with the accumulation of hydrogen peroxide close to disintegrating arbuscules (Fester and Hause, 2005).

The analysis of metabolic flux and regulation in specialized nongreen plastids in recent years has provided crucial features of metabolism in these organelles. In short, the oxidative PPP can be assumed to be the main source for NADPH as has been shown in a number of studies regarding Glu biosynthesis (Bowsher et al., 1989, 1992; Wright et al., 1997; Esposito et al., 2003). The intermediates of the oxidative PPP and glycolysis have been shown to be rapidly exchangeable between plastids and the cytosol when analyzing fatty acid producing *Brassica napus* embryos (Schwender et al., 2004). ATP-consuming pathways, like the methylerythritol-P pathway necessary for carotenoid biosynthesis, are mainly controlled by the activity of the ATP translocator in the inner plastid envelope as has been shown for starch biosynthesis in potato (*Solanum tuberosum*) tubers (Geigenberger et al., 2004). Furthermore, it is tempting to speculate that phosphate provided by the fungus might have a direct influence on the various translocators situated in the inner plastid envelope and on starch biosynthesis (Douds et al., 2000), leading to a higher level of glycolytic intermediates within the cytosol. Thus, the provision of high amounts of phosphate by the fungus might be ultimately linked to an elevated amount of carbohydrates available for the fungus.

Cytological Changes during Arbuscule Formation

Regarding mitochondria, Logan and Leaver (2000) described shapes ranging from spherical to sausage- or thread-like forms for roots from Arabidopsis (*Arabidopsis thaliana*). In *M. truncatula* as in Arabidopsis, spherical forms appear to be more predominant within root cortical cells, whereas thread-like forms are abundant in the central cylinder. Nevertheless, there is a certain percentage of thread-like mitochondria in root cortical cells from *M. truncatula*. Upon colonization of root cortical cells, mitochondria are aggregating in the vicinity of arbuscules forming clumps similar to those reported by Logan and Leaver (2000) for cells from the Arabidopsis hypocotyl.

Plastids in the roots of *M. truncatula* show a wide range of structural variation: Plastids from the cortex of root explants have a very large, amyloplast-like appearance without possessing any stromules, and plastids from the root cortex of intact plants are much smaller, but apparently free of stromules as well. Stromules become visible in the case of plastids from the central cylinder, from root nodules (B. Hause, K. Demchenko, and K. Pawlowski, personal communication), and from root cortical cells colonized by AM fungi. Plastids from root nodules and from arbusculated root cortical cells do not only share structural features, but some metabolic features as well. According to a metabolite and transcript profiling project for the rhizobial interaction of *L. japonicus*, another member of the *Fabaceae*, plastids from root nodules are mainly involved in the biosynthesis of amino acids, most notably Asn, which is the major export form of nitrogen from the nodules of *L. japonicus* and *M. truncatula* (Colebatch et al., 2004). Similarities regarding this metabolic pathway are further suggested by our electronic northern analysis. cDNA libraries from mycorrhizal and nodulated roots show similar numbers of EST clones connected to Asn or Asp metabolism, which is not the case for sequences connected to fatty acid biosynthesis or apocarotenoid accumulation. Plastid stromule formation has been suggested to be linked to increased metabolic activity of plastids (e.g. Kwok and Hanson, 2004; Waters et al., 2004). Such

a correlation seems to be supported by the examples presented above.

There are several possible reasons for the correlation of plastid metabolic activity and stromule formation. Stromules allow the plastids of a given cell to physically interact with each other. In the case of arbusculated cells from *N. tabacum* and *Z. mays*, plastids seem to form one large compartment, covering the growing arbuscule in a net-like appearance. In the case of *M. truncatula*, this interconnection is somewhat less pronounced. In addition, an increase in the area of the plastid inner envelope may be necessary for the exchange of plastid metabolites and in particular for the biosynthesis of lipophilic compounds, like fatty acids and carotenoids. A possible connection between carotenoid biosynthesis and stromule formation in AM roots is suggested by a comparison of these features in *M. truncatula* on one hand and in *N. tabacum* and *Z. mays* on the other. Both the activity of carotenoid biosynthesis (Fester et al., 2002a, 2002b) and of stromule formation appear to be decreased in *M. truncatula* when compared with these two plants.

Outlook

The use of organelle-targeted GFP and the complementary results regarding transcript and metabolite levels provided a first general overview of structural and metabolic changes of cell organelles during colonization by AM fungi. To our knowledge, the magnitude and extent of these changes are not paralleled by other biological processes involving root plastids. A detailed functional analysis of the formation of plastid networks in AM roots might reveal factors involved in signaling between nucleus and plastids, between individual plastids, and between the plant and the fungal cell. The data presented here define possible markers for such an analysis regarding metabolic changes. Similar markers for the study of structural changes are currently being studied (e.g. the plastid division protein FtsZ; Osteryoung and McAndrew, 2001) or still have to be determined (e.g. genes involved in stromule formation).

MATERIALS AND METHODS

Plant Material and AM Fungus Inoculation

Barrel medic (*Medicago truncatula* L. Gaertn. var Jemalong) was grown in a greenhouse in pots filled with expanded clay (Lecaton, 2–5 mm particle size; Fibo Exclay Deutschland). Seven-day-old seedlings (five plants per 500-mL pot) were inoculated with the AM fungus *Glomus intraradices* Schenck and Smith by the application of propagules in expanded clay (isolate 49, provided by H. von Alten from the collection of the Institut für Pflanzenkrankheiten und Pflanzenschutz der Universität Hannover, Germany). Further details of plant growth conditions have been described previously (Maier et al., 1995). Roots were harvested at 30, 60, or 90 d after inoculation. Part of the root system from each pot was used for the estimation of approximate colonization percentage (colonized roots/whole root system) according to Philips and Hayman (1970) after staining with trypan blue in lactophenol. The rest of the roots was homogenized in liquid nitrogen and stored at −80°C.

Root Transformation and Microscopy Analysis

Roots of *M. truncatula* were transformed according to the method published by Boisson-Dernier et al. (2001) using the *Agrobacterium rhizogenes* strain ARquaI. A construct containing the signal peptide of spinach (*Spinacia oleracea*) ferredoxin NADP(H) oxidoreductase fused to a modified version of the GFP cloned in pBIN (kindly provided by R.B. Klösgen, Halle, Germany; for further description, see Marques et al., 2004) was used for targeting the GFP to plastids. A similar construct in pSMAB701 containing the signal peptide of the γ-subunit of the Arabidopsis (*Arabidopsis thaliana*) mitochondrial F_1-ATPase (kindly provided by Y. Niwa, Shizuoka, Japan; for further description, see Niwa et al., 1999) was used for targeting a modified version of the GFP (S65T-GFP) to mitochondria. Composite plants with transformed roots were selected by fluorescence stereomicroscopy (using the GFP1-filter of the MZ FLIII from Leica) before being planted into open pots filled with expanded clay and the mycorrhizal inoculum (*G. intraradices* Schenck and Smith). Hairy root explants were prepared by repeated subculturing of transformed roots, first in liquid culture containing 1 mg mL^{-1} augmentin, then on agar plates containing the same amount of the antibiotic. The composite plants were accustomed to greenhouse conditions and harvested after approximately 8 weeks. Transformed roots were selected again by fluorescence stereomicroscopy, sliced with a razor blade, and immediately analyzed by CLSM. CLSM was performed using the LSM 510 Meta from Zeiss equipped with a Kr/Ar laser (emission at 488 nm). GFP fluorescence (filter setting: NFT545, BP505–530), orange red autofluorescence of root cell walls and arbuscules (filter setting: NFT545, LP560), as well as bright-field micrographs were collected simultaneously.

In Silico Analysis of Gene Expression

TC sequences corresponding to enzymes from various metabolic pathways were searched using the respective lists provided by the TIGR *Medicago truncatula* Gene Index (MtGI Release 7.0; http://www.tigr.org/tdb/tgi/mtgi/). TC and clone identification numbers are further given according to the MtGI nomenclature. The numbers of ESTs constituting the TC sequences were compared in three cDNA libraries from mycorrhizal roots (MHAM, MTAMP, MTBC; comprising 19,366 EST clones) on the one hand, and five libraries from nonmycorrhizal roots (MTBA, KVO, MTRHE, rootphos-, developing root; comprising 18,783 EST clones) on the other hand. The likelihood ratio (R) between the two hypotheses that a given gene is differentially expressed (H^1) and that it is not differentially expressed (H^0) was calculated for every TC sequence analyzed according to Equations 4 and 8 from Journet et al. (2002). TC sequences with R = 1.7 and higher were aligned against their most similar tentative annotations as given by MtGI or as found by BLAST homology search using the BLAST algorithm (http://www.ncbi.nlm.nih.gov/BLAST/). Details of annotation are given online in Supplemental Table I. For estimating transcript levels of these TC sequences in nodulated roots, the number of respective EST clones in the libraries MtSN4, GVN, GVSN, *M. truncatula* R108 Mt, nodulated root, and MtBB (comprising 21,373 sequences in total) were counted.

Analysis of Transcript Steady-State Levels

Total RNA was extracted from roots using a modified protocol from Gibco BRL Life Technologies. Ground, frozen root material (100 mg) was suspended in 1 mL TriReagent (Sigma-Aldrich). After centrifugation, the supernatant was extracted with chloroform, and RNA was precipitated by adding 250 μL 0.8 M sodium citrate, 1.2 M sodium chloride, and 250 μL isopropanol to 450 μL solution. The RNA pellet was washed twice with 75% (v/v) ethanol, dissolved in 20 μL water, and analyzed photometrically and by nondenaturing agarose/ethidium bromide gel electrophoresis. cDNA was synthesized using Moloney murine virus reverse transcriptase (Promega) according to the instructions from the manufacturer.

Primers for real-time PCR analysis were designed for all TC sequences showing R-values >1.7 using Primer Express software (Applied Biosystems). Prior to primer design, the parts of the TC sequences without homology to the coding sequence of the most similar tentative annotation were deleted. When comparing primer pairs with the MtGI database, six primer pairs recognized closely related TC sequences annotated to the same enzymes. In all other cases, primer pairs recognized only the TC sequence they had been derived from. The primers used for analysis are given online in Supplemental Table II.

Real-time PCR was performed using an Applied Biosystems Prism 7000 sequence detection system according to the instructions from the manufacturer. Amplification was followed using the dye SYBR Green I in assays with

a total volume of 20 μL. The quality of primers and the efficiency of the amplification were checked by conventional PCR, by analyzing the melting behavior of the PCR product after real-time PCR, and by running standard curves using five different dilutions (factor 4) of cDNA. All assays (standard curve and measurements) were run with three technical parallels. For each transcript studied, three biologically independent samples from mycorrhizal and nonmycorrhizal roots were measured, respectively, summing up to 18 assays per transcript. The data were evaluated using the comparative C_T method for relative quantitation as specified by Applied Biosystems. Δc_t-values were calculated by subtracting mean c_t-values of assays from mycorrhizal roots from the respective mean c_t-values of assays from nonmycorrhizal roots. The analysis was performed twice using two different plant batches harvested 60 d after inoculation. Amplicons showing high Δc_t-values were then analyzed again using roots harvested 30 and 90 d after inoculation, respectively. An amplicon corresponding to TC85208 (annotated to the translation elongation factor 1α; 5′-AGCACCAAGCAAAGCATCCT-3′, 5′-AGGTTGTTACTCGTTCGGATCCT-3′) was used as an endogenous control and an amplicon corresponding to the *M. truncatula* phosphate transporter 4 (AY116210; Harrison et al., 2002; 5′-ACAAATTTGATAGGATTCTTTTGCACGT-3′, 5′-TCACATCTTCTCAGTTCTTGAGTC-3′) as a positive control. $\Delta\Delta c_t$-Values were calculated by substracting the Δc_t-value for the constitutively expressed translation elongation factor 1α from the Δc_t-values of the various samples. cDNA assays without reverse transcriptase (RT^-) were used as a control for a possible amplification of contaminating DNA material. We only evaluated samples when these real-time PCR assays either gave no amplification or when the weak signals eventually observed accounted for $<$2% of the template measured in nonmycorrhizal roots.

Analysis of Nonpolar Metabolite Steady-State Levels

Roots of *M. truncatula* were harvested 40 d after inoculation with *G. intraradices*. After addition of 15 μL methyl nonadecanoate (0.2 mg mL^{-1} $CHCl_3$, internal standard), lyophilized roots (30 mg) were homogenized in a mortar with addition of solid CO_2 and extracted three times with 0.5 mL hexane. Aliquots of the extracts were derivatized using *N*-methyl-*N*-(trimethylsilyl)-trifluoroacetamide (30 min, 70°C) after reducing to dryness. Metabolites were separated and analyzed using a gas chromatograph (Agilent 6890) equipped with a TOF-MS (GCT; Waters). Column specifications are as follows: DB-5 MS 30 m $\times$ 0.25 mm, i.d.; 0.25-μm film thickness; carrier gas, helium at constant flow 1 mL min^{-1}; temperature program, 2 min 50°C, then 10°/min to 300°, 10 min 300°, 10°/min to 320°, 11 min at 320°. Splitless injection was as follows: 1 μL at 250°; mass-to-charge ratio 40 to 800.

Analysis of Polar Metabolite Steady-State Levels

Metabolites were extracted according to Roessner et al. (2000) with the following modifications. Aliquots of ground root samples were mixed with 360 μL methanol (−20°C) plus 30 μL ribitol in methanol (0.2 mg mL^{-1}) and 30 μL d_4-Ala in water (1 mg mL^{-1}). Samples were shaken for 15 min at 70°C before addition of 200 μL chloroform and further shaking at 37°C for 5 min. After addition of 400 μL water, samples were vortexed, then centrifuged at 21,000*g* for 5 min at room temperature. Two 80-μL aliquots of the aqueous phase were transferred to Eppendorf tubes and dried at room temperature by vacuum centrifugation (Centrivac; Heraeus). Metabolite derivatization was performed according to Roessner et al. (2000) with the following modifications. One of each pair of dried samples was resuspended in 40 μL methoxyamine hydrochloride (20 mg mL^{-1} in pyridine) at 30°C for 90 min and 70 μL *N*-methyl-*N*-(trimethylsilyl)-trifluoroacetamide plus 10 μL alkane mixture (see below). GC-MS spectra were obtained with a GC8000 gas chromatograph coupled to a Voyager quadrupol-type mass spectrometer operated by MassLab software (ThermoQuest). Modifications to the initial GC-MS profiling method (Fiehn et al., 2000a, 2000b) included injection of a 1-μL sample in splitless mode, use of a 5°C min^{-1} temperature ramp with final temperature set to 320°C on a 30 m $\times$ 0.25 mm i.d. Rtx-5Sil MS capillary column with an integrated guard column (Restek), and use of the C_{12}, C_{15}, C_{19}, C_{22}, C_{32}, and C_{36} *n*-alkane mixtures for the determination of retention time index. Metabolites were identified and quantified as detailed by Colebatch et al. (2004).

ACKNOWLEDGMENTS

The authors thank Dr. J.P. Marques (Martin-Luther-University Halle-Wittenberg, Germany) and Dr. R.B. Klösgen (Martin-Luther-University Halle-Wittenberg, Germany) for kindly providing a transformation construct for targeting the GFP into plastids, Dr. Y. Niwa (University of Shizuoka, Japan) for a similar construct regarding the labeling of mitochondria, and Dr. P.A. Olsson (University of Lund, Sweden) for cooperation in identifying fatty acids.

Received February 16, 2005; revised June 2, 2005; accepted June 7, 2005; published August 26, 2005.

LITERATURE CITED

Bago BB, Pfeffer PE, Shachar-Hill Y (2000) Carbon metabolism and transport in arbuscular mycorrhizas. Plant Physiol **124:** 949–957

Boisson-Dernier A, Chabaud M, Garcia F, Bécard G, Rosenberg C, Barker DG (2001) *Agrobacterium rhizogenes*-transformed roots of *Medicago truncatula* for the study of nitrogen-fixing and endomycorrhizal symbiotic associations. Mol Plant Microbe Interact **14:** 695–700

Bonfante-Fasolo P (1984) Anatomy and morphology of VA mycorrhiza. *In* CL Powell, DJ Bagyaraj, eds, VA Mycorrhiza. CRC Press, Boca Raton, FL, pp 5–33

Bowsher CG, Boulton EL, Rose J, Nayagam S, Emes MJ (1992) Reductant for glutamate synthase is generated by the oxidative pentose phosphate pathway in non-photosynthetic root plastids. Plant J **2:** 893–898

Bowsher GC, Hucklesby DP, Emes MJ (1989) Nitrite reduction and carbohydrate metabolism in plastids purified from roots of *Pisum sativum* L. Planta **177:** 359–366

Colebatch G, Desbrosses G, Ott T, Krusell L, Montanare O, Kloska S, Kopka J, Udvardi MK (2004) Global changes in transcription orchestrate metabolic differentiation during symbiotic nitrogen fixation in *Lotus japonicus*. Plant J **39:** 487–512

Douds DD, Pfeffer PE, Shachar-Hill Y (2000) Carbon partitioning, cost and metabolism of arbuscular mycorrhizae. *In* Y Kapulnik, DD Douds, eds, Arbuscular Mycorrhizas: Physiology and Function. Kluwer Academic Press, Dordrecht, The Netherlands, pp 107–130

Esposito S, Massaro G, Vona V, Di Martino Rigano V, Carfagna S (2003) Glutamate biosynthesis in barley roots: the role of the plastidic glucose-6-phosphate dehydrogenase. Planta **216:** 639–647

Fester T, Hause G (2005) Accumulation of reactive oxygen species in arbuscular mycorrhizal roots. Mycorrhiza **15:** 373–379

Fester T, Hause B, Schmidt D, Halfmann K, Schmidt J, Wray V, Hause G, Strack D (2002a) Occurrence and localization of apocarotenoids in arbuscular mycorrhizal plant roots. Plant Cell Physiol **43:** 256–265

Fester T, Schmidt D, Lohse S, Walter MH, Giuliano G, Bramley PM, Fraser PD, Hause B, Strack D (2002b) Stimulation of carotenoid metabolism in arbuscular mycorrhizal roots. Planta **216:** 148–154

Fester T, Strack D, Hause B (2001) Reorganization of tobacco root plastids during arbuscule development. Planta **213:** 864–868

Fester T, Wray V, Nimtz M, Strack D (2005) Is stimulation of carotenoid biosynthesis in arbuscular mycorrhizal roots a general phenomenon? Phytochemistry **66:** 1781–1786

Fiehn O, Kopka J, Dörmann P, Altmann T, Trethewey RN, Willmitzer L (2000a) Metabolite profiling for plant functional genomics. Nat Biotechnol **18:** 1157–1161

Fiehn O, Kopka J, Trethewey RN, Willmitzer L (2000b) Identification of uncommon plant metabolites based on calculation of elemental compositions using gas chromatography and quadrupole mass spectrometry. Anal Chem **72:** 3573–3580

Geigenberger P, Stitt M, Fernie AR (2004) Metabolic control analysis and regulation of the conversion of sucrose to starch in growing potato tubers. Plant Cell Environ **27:** 655–673

Gianinazzi-Pearson V (1996) Plant cell responses to arbuscular mycorrhizal fungi: getting to the roots of the symbiosis. Plant Cell **8:** 1871–1883

Hans J, Hause B, Strack D, Walter MH (2004) Cloning, characterization, and immunolocalization of a mycorrhiza-inducible 1-deoxy-*D*-xylulose 5-phosphate reductoisomerase in arbusule-containing cells of maize. Plant Physiol **134:** 614–624

Harrison MJ, Dewbre GR, Liu J (2002) A phosphate transporter from *Medicago truncatula* involved in the acquisition of phosphate released by arbuscular mycorrhizal fungi. Plant Cell **14:** 2413–2429

Hause B, Fester T (2004) Molecular and cell biology of arbuscular mycorrhizal symbiosis. Planta **221:** 184–196

Hodge A, Campbell CD, Fitter AH (2001) An arbuscular mycorrhizal fungus accelerates decomposition and acquires nitrogen directly from organic material. Nature **413:** 297–299

Imaizumi-Anraku H, Takeda N, Charpentier M, Perry J, Miwa H, Umehara Y, Kouchi H, Murakami Y, Mulder L, Vickers K, et al (2005) Plastid proteins crucial for symbiotic fungal and bacterial entry into plant roots. Nature **433:** 527–531

Isayenkov S, Fester T, Hause B (2004) Rapid determination of fungal colonization and arbuscule formation in roots of *Medicago truncatula* using real-time (RT) PCR. J Plant Physiol **161:** 1379–1383

Journet EP, van Tuinen D, Gouzy J, Crespeau H, Carreau V, Farmer MJ, Niebel A, Schiex T, Jaillon O, Chatagnier O, et al (2002) Exploring root symbiotic programs in the model legume *Medicago truncatula* using EST analysis. Nucleic Acids Res **30:** 5579–5592

Kwok EY, Hanson MR (2004) Stromules and the dynamic nature of plastid morphology. J Microsc (Oxf) **214:** 124–137

Liu J, Blaylock LA, Endre G, Cho J, Town CD, VandenBosch KA, Harrison MJ (2003) Transcript profiling coupled with spatial expression analyses reveals genes involved in distinct developmental stages of an arbuscular mycorrhizal symbiosis. Plant Cell **15:** 2106–2123

Logan DC, Leaver CJ (2000) Mitochondria-targeted GFP highlights the heterogeneity of mitochondrial shape, size and movement within living plant cells. J Exp Bot **51:** 865–871

Mackenzie S, McIntosh L (1999) Higher plant mitochondria. Plant Cell **11:** 571–585

Maier W, Peipp H, Schmidt J, Wray V, Strack D (1995) Levels of a terpenoid glycoside (blumenin) and cell wall-bound phenolics in some cereal mycorrhizas. Plant Physiol **109:** 465–470

Marques JP, Schattat MH, Hause G, Dudeck I, Klösgen RB (2004) *In vivo* transport of folded EGFP by the ΔpH/TAT-dependent pathway in chloroplasts of *Arabidopsis thaliana*. J Exp Bot **55:** 1697–1706

Niwa Y, Hirano T, Yoshimoto K, Shimizu M, Kobayashi H (1999) Non-invasive quantitative detection and applications of non-toxic, S65T-type green fluorescent protein in living plants. Plant J **18:** 455–463

Olsson PA (1999) Signature fatty acids provide tools for determination of the distribution and interactions of mycorrhizal fungi in soil. FEMS Microbiol Ecol **29:** 303–310

Osteryoung KW, McAndrew RS (2001) The plastid division machine. Annu Rev Plant Physiol Plant Mol Biol **52:** 315–333

Philips JM, Hayman DS (1970) Improved procedures for cleaning roots and staining parasitic and vesicular-arbuscular mycorrhizal fungi for rapid assessment of infection. Trans Br Mycol Soc **55:** 158–162

Roessner U, Wagner C, Kopka J, Trethewey RN, Willmitzer L (2000) Simultaneous analysis of metabolites in potato tuber by gas chromatography-mass spectrometry. Plant J **23:** 131–142

Schwartz SH, Qin X, Zeevaart AD (2001) Characterization of a novel carotenoid cleavage dioxygenase from plants. J Biol Chem **276:** 25208–25211

Schwender J, Ohlrogge J, Shachar-Hill Y (2004) Understanding flux in plant metabolic networks. Curr Opin Plant Biol **7:** 309–317

Smith SE, Read DJ (1997) Mycorrhizal Symbiosis, Ed 2. Academic Press, London

Strack D, Fester T, Hause B, Schliemann W, Walter MH (2003) Arbuscular mycorrhiza: biological, chemical and molecular aspects. J Chem Ecol **29:** 1955–1979

Walter MH, Fester T, Strack D (2000) Arbuscular mycorrhizal fungi induce the non-mevalonate methylerythritol phosphate pathway of isoprenoid biosynthesis correlated with accumulation of the ''yellow pigment'' and other apocarotenoids. Plant J **21:** 571–578

Waters MT, Fray RG, Pyke KA (2004) Stromule formation is dependent upon plastid size, plastid differentiation status and the density of plastids within the cell. Plant J **39:** 655–667

Wright DP, Huppe HC, Turpin DH (1997) *In vivo* and *in vitro* studies of glucose-6-phosphate dehydrogenase from barley root plastids in relation to reductant supply for NO_2^- assimilation. Plant Physiol **114:** 1413–1419